

Recognizing Different Foot Deformities Using FSR Sensors by Static Classification of Neural Networks

Ayham Darwich^{1,2}  , Ebrahim Ismaiel^{*1}  , Ayman Al-kayal¹  , Mujtaba Ali¹  ,
Mohamed Masri¹  , Hasan Mhd Nazha³  

¹Faculty of Biomedical Engineering, Al-Andalus University for Medical Sciences, Tartous, Syria.

²Department of Industrial Automation, Faculty of Technical Engineering, University of Tartous, Tartous, Syria.

³Institute of Mechanics, Faculty of Mechanical Engineering, Otto Von Guericke University Magdeburg, Universitätsplatz, Magdeburg, Germany.

*Corresponding Author.

Received 19/04/2023, Revised 26/08/2026, Accepted 28/08/2023, Published 05/12/2023



This work is licensed under a [Creative Commons Attribution 4.0 International License](https://creativecommons.org/licenses/by/4.0/).

Abstract

Sensing insole systems are a promising technology for various applications in healthcare and sports. They can provide valuable information about the foot pressure distribution and gait patterns of different individuals. However, designing and implementing such systems poses several challenges, such as sensor selection, calibration, data processing, and interpretation. This paper proposes a sensing insole system that uses force-sensitive resistors (FSRs) to measure the pressure exerted by the foot on different regions of the insole. This system classifies four types of foot deformities: normal, flat, over-pronation, and excessive supination. The classification stage uses the differential values of pressure points as input for a feedforward neural network (FNN) model. Data acquisition involved 60 subjects diagnosed with the studied cases. The implementation of FNN achieved an accuracy of 96.6% using 50% of the dataset as training data and 92.8% using only 30% training data. The comparison with related work shows good impact of using the differential values of pressure points as input for neural networks compared with raw data.

Keywords: Foot deformities, feedforward neural network, human gait, resistive pressure sensor, sensing insole.

Introduction

Walking stability is known as the gait pattern that does not cause falling or stumbling. It is accomplished by all the anatomical elements and the integrity of the neuromuscular system, which is responsible for movement orders modified according to human movement parameters ¹. The stability of human gait is affected by the position of the body's center of mass (COM) according to the support base, which expresses the area of the foot that contacts the floor. Gait stability also depends on the biomechanics of the body which can involve: a large mass position lying in a high area versus a small support area; any minor deviation in the anatomical

structure of the foot may appear as a variation of the gait acceleration; and a rapid change in the position of the COM ending with stumbling and falling ². Therefore, abnormal gait patterns and patient movement can be caused by abnormal changes in the shape of the foot and enforce the patient to exert more energy to perform his daily tasks ³. The foot is prone to many deformities ⁴ where it can be flat or inclined on the medial, or lateral side or deformities in its arch. These deformities normally originated from congenital causes, an accident, or caused by improper loading ⁵. There is increasing suffering from chronic pain in the foot caused by a flat foot ⁶.

In addition to inheritance, foot abnormalities could be originated from several factors such as the type of shoes, overweight, and body fitness⁷. The stability of the human gait cycle is controlled through the right positioning of the foot, which represents the main condition for moving forward, and it also helps in stabilizing the body based on inertial dynamics. Normal foot conditions can be defined in terms of a good alignment of the feet and ankles. In this case, loading pressure could be evenly distributed on foot area⁸. The presence of medium, high, low, or completely collapsed arches disrupts the distribution of body weight across the foot, impairing shock absorption and causing constrained foot stretching and tension⁹. Feet can be classified into three general categories based on how they absorb the shock and propel the body forward¹⁰. Low or collapsed arches are often related to overpronation, while high arches are often associated with excessive supination. Overpronation can also occur with high arches. Flat Foot distortion represents flattened arches on the bottom of the foot and is caused by a weakness of the abrasive muscles and congenital foot surface¹¹.

Diabetic foot and foot deformities are diagnosed by simple radiography¹² computed tomography¹³, or magnetic resonance imaging (MRI)¹⁴. Although these methods are very common due to their high accuracy in determining the nature of the deformity, they are expensive and require complex work systems¹⁵. In contrast, non-radial systems, such as force plates or sensors need simple installation, and they are easy to install on patient¹⁶. Recently, due to tremendous continuous technological advancement, several devices and sensors have been developed to facilitate the medical analysis of the applied pressure of the foot based on the sensing insole. These systems can be used for long-term or real-time patient monitoring¹⁷.

Force sensitive resistors (FSRs) are sensors that change their resistance according to the applied force or pressure. They can be used for gait assessment by measuring the underfoot pressures during different phases of walking or running. FSR-based insoles have been used in many foot biomechanics systems (FBSs) as low-cost acquisition systems¹⁸.

Fazio *et al.* presented a pressure sensor array that incorporated a Velostat electrostatic-sensitive layer to convert applied pressure into an electrical signal. The provided insole is based on a 3-axis capacitive accelerometer to measure patient gait parameters (during swing and stance phases). While the system

demonstrated the feasibility of using pressure sensors and accelerometers for gait analysis, its accuracy may be limited by the use of only one type of sensor¹⁹. In contrast, the proposed system uses a combination of FSRs and accelerometers, which can provide more accurate and comprehensive data on foot biomechanics.

Wang *et al.* used an array structure of pressure sensors to analyze standing and walking during normal and sports movement activities²⁰. The study highlighted the possible use of high-frequency pressure sensors and the acquired values have shown an accuracy of 92%. While the system demonstrated high accuracy, the use of high-frequency pressure sensors may limit the system's applicability to specific scenarios. In contrast, the proposed system uses FSRs, which are low-cost and can be used in various situations.

Park *et al.* presented a new design of foot insole with high-sensitive stress sensors that consisted of industrial rubber, stainless steel, and a 3D-printed frame²¹. The device was able to distinguish the distribution of the load on the whole surface of the foot. While the system demonstrated high sensitivity and durability, the use of industrial rubber and stainless steel may limit the system's flexibility and comfort for the wearer. In contrast, the proposed system uses soft and flexible materials, which can provide more comfort and flexibility for the wearer. Suprpto *et al.* used a structure of double electrode sensors on the upper and lower part of a layer of Valdosta material²². Experimental results showed that the force sensors array has a linear response to electrical conductivity. While the system demonstrated the feasibility of using double electrode sensors for force measurement, the use of Valdosta material may limit the system's applicability to specific scenarios. In contrast, the proposed system uses FSRs, which can be used in various situations. Ló *et al.* implemented a new design of a smart insole for real-time plantar pressure measurement²³. The recorded pressure values had an accuracy of 93%, pressure sensors were calibrated, and the results were compared to a Kistler system. While the system demonstrated high accuracy, the use of a Kistler system for comparison may limit the system's applicability to specific scenarios. In contrast, the proposed system uses a combination of FSRs and accelerometers, which can provide more accurate and comprehensive data on foot biomechanics.

These approaches highlighted in the previous works have their own strengths and weaknesses in terms of accuracy, sensitivity, durability, flexibility, and applicability to specific scenarios. The proposed system using FSRs and accelerometers can provide a low-cost and comprehensive solution for gait assessment and foot biomechanics, with potential applications in sports, rehabilitation, and footwear design.

On the other hand, advanced devices with many sensors and long-term data tracking require an automated software system that relies on the experience of doctors and specialists to process the data and give an immediate diagnosis of the situation²⁴. Hence comes the need for the use of machine learning (ML) and artificial intelligence (AI) techniques with a robust data set for training and validation. Lately, a lot of research work has used AI and ML techniques to diagnose the recorded pressure values from sensors-based foot insoles. Density-based spatial clustering with noise (DBSCAN) and K-means clustering techniques are used to extract gait features in cardiac stroke patients and evaluate their performance by comparing them with healthy people²⁵. Fine-tuned visual geometry group-16 (VGG16) and K-nearest neighbor (k-NN) models are combined to classify foot deformities based on numerical foot pressure data. The results show better performance compared to individual models that were built using the same numerical data²⁶. K-NN algorithm with FSR-based sensing insole was able to estimate the type of footprint biomechanics in preschool and school children volunteers with a classification accuracy of 97.2%, where the foot types were normal, flat, and arched²⁷. A long short-term memory (LSTM) model is used with numerical data from nine major sensors to evaluate the clinical rehabilitation status of feet. By comparing the performance of the LSTM with an adaptive neuro-fuzzy interference system (ANFIS) using correlation coefficient and relative root mean square error, LSTM proved its efficiency in estimating pressure distribution of the whole foot region with correlation coefficients of 0.92 to 0.99²⁸. A one-dimensional convolutional neural network (1D-CNN) can be used to detect normal, cavus, and planus feet using numerical data of nine force sensors of type FlexiForce. The neural network shows an accuracy of 99.26% by combining angular velocity and force sensing²⁹. Support Vector Machines and artificial neural networks were combined to classify the foot deformity based on the Velostat sensors matrix. The

proposed method can detect normal, high-arched, or low-arched with 95% accuracy³⁰. On the other hand, the SVM classifier reaches good accuracy of classification with an F1-score equal to 92.1% where the numerical data is integrated between inertial and plantar pressure sensors³¹. Eight force-sensing resistors were used as input for cascade neural networks with node-decoupled extended Kalman filtering (CNN-NDEKF) to detect the gait pattern associated with postural kyphosis³².

Accordingly, the foot deformity diagnostic systems that use sensor-based insoles and ML techniques use the direct numerical values of pressure recordings which lead to an accuracy of 70-95%²⁸⁻³¹.

The non-radial systems such as pressure plates and sensing insoles become more reliable and efficient diagnostic tools for most clinicians and specialists because of their simple installation and the ability of home use by the patients¹⁶. These systems can be used for long-term and real-time patient monitoring. Machine learning and artificial intelligence came to convert those types of medical examination tools into effective diagnostic tools for clinicians, orthotists, and prosthetists, and consider those portable devices as medical decision support systems. The long-term objective is to produce a smart insole that can measure and analyze the pressure distribution on the foot using capacitive pressure sensors. This system can provide valuable information about the balance, posture, gait, and risk of falls of the patients. The smart insole can also transmit the data wirelessly to a computer or a mobile device for further processing and visualization. ML and AI techniques can be applied to the data to extract meaningful features, identify patterns, classify different activities, detect anomalies, and provide feedback or recommendations. These techniques can enhance the accuracy, efficiency, and usability of the smart insole system as a medical decision-support tool.

This paper presents an electronic system to record foot pressure values from FSR sensors placed on the bottom of the insole. The measuring system was calibrated by placing the FSR between beneath the calibrated weights. The recorded values from the FSR were used as reference values for the regression process to find a mathematical model that relates the force to the voltage output of the FSR. Then enhance the classification of foot deformities by studying the effect of using the differential values between sensors as input for the feedforward neural network (FNN) instead of the raw data based on calculating

the difference between the sensors value and the value of the most influencing sensor. Finally, the findings illustrate the performance of FNN with raw

Materials and Methods

In this section, the used tools in this study is presented starting from hardware and sensor, collecting data, calibrating and validating recorded data, and finally classifying the foot deformities and illustrating the performance metrics.

Hardware implementation and calibration

The selection of appropriate sensors is essential for obtaining accurate and reliable measurements of foot biomechanics in the proposed system. The rationale behind the selection of sensors and the calibration procedures employed in this study are based on the principles of low cost, high sensitivity, ease of integration, and accuracy. The Interlink Electronics 402 FSRs are a cost-effective and reliable option for measuring foot pressure distribution. The calibration system used in this study provides a reproducible and reliable solution for obtaining accurate and reliable measurements of force and pressure. They represent single-zone sensors with a diameter of 12.7 mm. The FSRs are low-cost, highly sensitive, and easy to integrate with the Arduino platform. The size of the FSRs is appropriate for measuring the pressure distribution of the foot, and the single-zone design allows for a simpler and more compact sensor array. The FSRs are connected to an Arduino Mega platform, which is used to interface the sensors and record their corresponding voltage values³³. The Arduino system transmits voltage values to a computer via the wireless module, with a sampling rate of 200 Hz and a resolution of 10 bits. The rationale of sensor placement and protocol specification are described in Mei *et al.*²⁹.

The calibration of FSRs is essential for obtaining accurate and reliable measurements of force and pressure. The calibration system used in this study consists of a voltage-to-current converter circuit, a rigid dome coating, a load cell, and a data acquisition card. The circuit, shown in Fig. 1, converts the resistance value of the FSR into an inverse voltage output, ranging from 0 V to V_{REF} . The value of the RM resistor is chosen according to the recommendation to optimize the sensitivity and limit the current in the sensor³⁴. The dome coating is made of fiberglass resin and has a diameter of 12.7 mm and a thickness of 3.3 mm. It is attached to the sensor

and differential numerical input by training and testing the FNN with different accuracy measures and using different amounts of data.

using double-sided tape to distribute the force evenly over the sensor surface and to prevent saturation from punctual loads. The load cell is a calibrated device that measures the force applied to the sensor with high accuracy³⁵.

The calibration procedure involves applying a range of known forces to the sensor using the load cell and recording the corresponding voltage values. The recorded data are then used to construct a calibration curve that relates the voltage output of the sensor to the applied force. The calibration curve can then be used to convert the voltage values recorded by the Arduino system into force and pressure values in real-time.

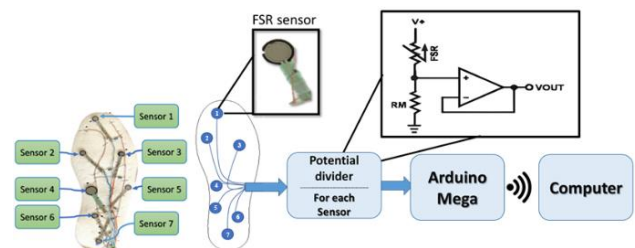


Figure 1. The proposed electronic system with the FSR-based insole and acquisition circuit

The calibration procedure involves placing the FSR between beneath the calibrated weights, which applies a controlled force. The voltage output from the FSR is acquired by the Arduino and sent to the computer to be stored in a spreadsheet file. The force values from the FSR are used as reference values for the regression process, which aims to find a mathematical model that relates the force to the voltage output of the FSR.

Data collection

This study involves 60 participants who were individually asked to make sessions with duration of 60 seconds where every 15 participants were clinically diagnosed with the following cases: Normal, flat foot, excessive pronation, and excessive supination. The study involved measuring static foot loading and assessing the foot topology. Each subject wore shoes with sensor insole. The data from the insole were transmitted wirelessly to a computer and analyzed using custom software. Subjects with pain

or injury in a foot, ankle, or knee, or who underwent surgery in these areas within the last six months before the experiment were excluded.

The Data recording procedure were conducted based on the Declaration of Al-Andalus University Hospital, Tartous, Syria and the announcement of patients by specialists. The measurements are conducted on 60 subjects who had been diagnosed previously by specialized doctors with following cases: Normal, flat foot, excessive pronation, and excessive supination. The age of participants ranged from 20 to 25 years and their weight range was 70-75 kg.

Each participant was informed about the experiment in addition to the necessary consent forms. Before the experiment, each participant was asked to fill out a form about age, gender, height, weight, and health status related to motor function. All participating subjects hadn't suffered pain or injury in the foot, ankle or knee and hadn't undergone any surgery in their lower limbs during the past year prior to data collection. Foot pressure data were recorded for each subject during a period of 60 sec. All participants received written and oral information about the measurements. The participants provided written informed consent before the start of the measurements. The study was registered in the Al-Andalus University Hospital Trials Register (AUHTR0002248). In this study, only the values of right foot were considered since the gait is symmetric between two feet.

Sensors values reliability

To compare the performance of the different sensors, the mean and standard deviation (SD) of the five repetitions for each sensor value were calculated. Then, a One-Way ANOVA test was implemented using IBM SPSS Statistics (Version 27) to examine the effect of the sensor type and the foot deformity on the sensor values. A significance level of 0.05 was used to determine if there were any statistically significant differences between the sensors and the cases.

Weight distribution and postural stability

The footprint index (FPI) is a widely used tool to measure foot posture and identify different foot types. It is based on the rate of non-contacted to the contacted area of the foot, reflecting the shape and alignment of the foot³⁶. In this study, the FPI was applied to examined subjects with various foot

conditions. The variations of this index were used to classify the subjects into four categories: Normal, flat foot, extra-pronation, and extra-supination. The results were compared with the different indices and evaluated their reliability and validity for foot typology assessment.

Foot deformities classification

The estimated dataset contains 60 records, each record contains seven values derived from the seven sensors and the eighth value refers to the pre-diagnosed foot case. In pre-processing, the differential values were computed and replaced with the raw data of sensors as shown in Fig. 2. The principle of differential data depends on calculating the difference between each sensor value and the value of the fifth sensor which is considered the most influenced sensor in all cases as shown in Fig. 3 in the results section. Furthermore, the position of sensor five represents the pressure value of the spleen part with the foot liver which is more sensitive to a lot of foot deformities³⁶. The classification procedure of the dataset is accomplished using FNN, which is a type of artificial neural network that has no feedback or closed loop between nodes or layers. It is often referred to as a multi-layered network of neurons. The FNN consists of an input layer of neurons, several hidden layers, and an output layer³⁶. The FNN was implemented using MATLAB (MathWorks, Natick, MA, United States) according to the following specifications: the input layer contains 7 nodes, the output layer contains a node (case type), the size of the hidden layer equals 3, the desired final performance value (10^{-8}), and the number of iterations 500. The different ratio between training and testing samples was used to evaluate the efficiency of using differential input and the stability of FNN performance with the reduced number of training data.

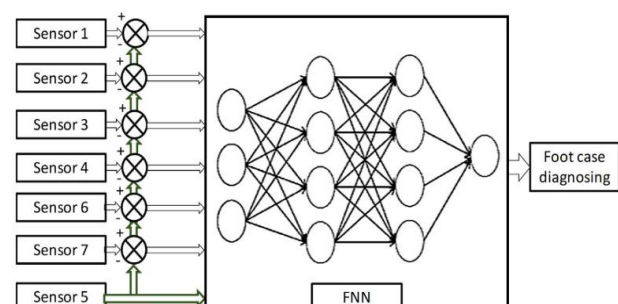


Figure 2. FNN network with differential input where the difference of each sensor is calculated based on the value of sensor five

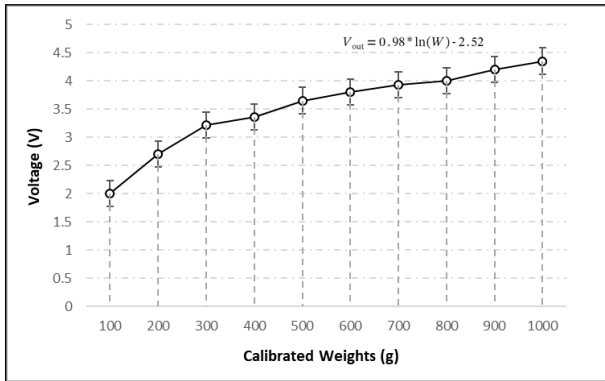


Figure 3. Calibration curve of FSR sensors using different weights

Performance measures

The performance is measured using a formula of accuracy (AC) (Eq. 1) and F1-score (Eqs. 2-4):

$$Accuracy = \frac{TP + TN}{TP + TN + FP + FN} \quad (1)$$

Results

Here, the final collected data is presented, starting from validating the sensor calibration, then detecting deformities using FSR and graphed data. Finally, illustrates the classification results using the FNN network.

Sensor calibration

To achieve an efficient sensor calibration process, many reference weights were applied on the insole and then build up Eq. 5 based on the corresponding changes.

$$V_{out} = 0.98 \ln(W) - 2.52 \quad (5)$$

Where V_{out} is the output voltage, W is the applied weight. The outcomes of calibration in terms of the output voltage versus the applied weight are shown in Fig. 3. The figure also shows the equation of logarithmic fit, showing a high degree of accuracy for the calibration process.

Sensor values reliability

One-Way ANOVA test showed that both the main effects of the cases and the sensors were significant, as well as the interaction effect between them. This means that the values of the sensors varied depending on the case, and that some sensors were more sensitive to the changes in the cases than others. To

$$F1 - score = \frac{2 \times Precision \times Recall}{Precision + Recall} \quad (2)$$

$$Precision = \frac{TP}{TP + FP} \quad (3)$$

$$Recall = \frac{TP}{TP + FN} \quad (4)$$

Where:

True Positive (TP): The number of correctly classified data indicating the correct case. False Positive (FP): The number of incorrectly categorized data that is not indicative of the correct case. True Negative (TN): The number of data classified as not the correct case and not indicative of the case. False Negative (FN): The number of data classified as not the correct case and indicative of the case.

further investigate the differences among the sensor values for each case, posthoc tests were performed using Bonferoni method. The posthoc tests revealed which pairs of sensors had significantly different mean values for each case, with a significance level of 0.05. The results of the post-hoc tests are summarized in Table 1, where an asterisk indicates a significant difference. The values of sensor 1 and sensor 7 were excluded from the analysis, because they did not show any noticeable variation across the cases.

Weight distribution and postural stability

In the first step, a scale for weight distribution was built over the used sensors during the different studied foot deformities: normal, flat foot, pronation and supination (Table 2). Initially, weight was evenly distributed over the sensors during the normal case. However, the deformities can be recognized based on the variations of loading percentage values, giving an indication of sensor dominance or the area of deformity. For example, flat foot deformity is characterized by a higher voltage on the medial side of the foot (sensor 4), while supination deformity is characterized by a higher voltage on the lateral side of the foot (sensors 3, 5, 7).

Table 1. Sensors values reliability where the significance of values differences has been tested using one-way ANOVA at the different foot cases: N, normal; F: flat foot; S: Supination; P: Pronation

Studied Sensor	Studied case	Compared case	Mean Difference	Std. Error	Sig.
Sensor 2	N	F	.00	.21378	1.00
		S	-3.34*	.21378	.000
		P	2.32*	.21378	.000
Sensor 3	N	F	-.14	.13304	1.00
		S	.28	.13304	.309
		P	-6.52*	.13304	.000
Sensor 4	N	F	-3.40*	.11958	.000
		S	-2.56*	.11958	.000
		P	3.26*	.11958	.000
Sensor 5	N	F	.16	.15843	1.00
		S	1.26*	.15843	.000
		P	-4.40*	.15843	.000
Sensor 6	N	F	-.04	.22204	1.00
		S	-3.22*	.22204	.000
		P	2.72*	.22204	.000

Table 2. Weight distribution scale on the different sensors in the four studied cases

	Normal	Flat Foot	Pronation	Supination
r 1 sensor on Load	12%	11%	9%	12%
r 2 sensor on Load	14%	13%	22%	5%
r 3 sensor on Load	9%	9%	7%	27%
r 4 sensor on Load	18%	25%	22%	5%
r 5 sensor on Load	12%	11%	5%	28%
r 6 sensor on Load	17%	15%	21%	5%
r 7 sensor on Load	18%	16%	14%	18%

In the second step, the FPI index was used to differentiate between deformities based on the rate of uncontacted area of the foot to the whole foot contacted area. A clear difference was noticed between the four studied cases in addition to differentiating between foot deformities based on FPI variations. The results are shown in Table 3. The normal case has a FPI value of 30%, while the flatfoot case was characterized by a value of 5%. The pronation case is characterized by a FPI value of 15%, while the supination case has a FPI value of 50%. These findings suggest that FPI can be used as an objective and quantitative measure to classify foot deformities and monitor their progression over time.

Table 3. Foot print index variations in the four studied cases

	Normal	Flat Foot	Pronation	Supination
FP I	0.30±0.1	0.05±0.00	0.18±0.07	0.50±0.1

Deformities detection using FSR

The final records set contains 60 samples divided equally into four cases of foot types and each sample or record consists of seven values obtained from the sensors in “Volt” in addition to the label of the pre-diagnosed case from a clinician as the eighth value. The values of sensors concerning the four-foot cases are illustrated in Fig. 4 where each foot case is represented by the seven values. The normal foot has higher voltage in the outer part of the foot (Sensors 1, 2, 3, 5, 6, and 7). The flat foot tends to have more equal distribution over sensors compared with the normal foot. In the overpronation foot, the inner pressure point of the foot sole must be higher than the outer points which are clear in Fig. 3, where sensors (2, 4, and 6) are higher than the rest. In contrast, excessive supination shows higher voltage in the outer points of the foot sole as shown in Fig. 3 (sensors 1, 3, 5, and 7).

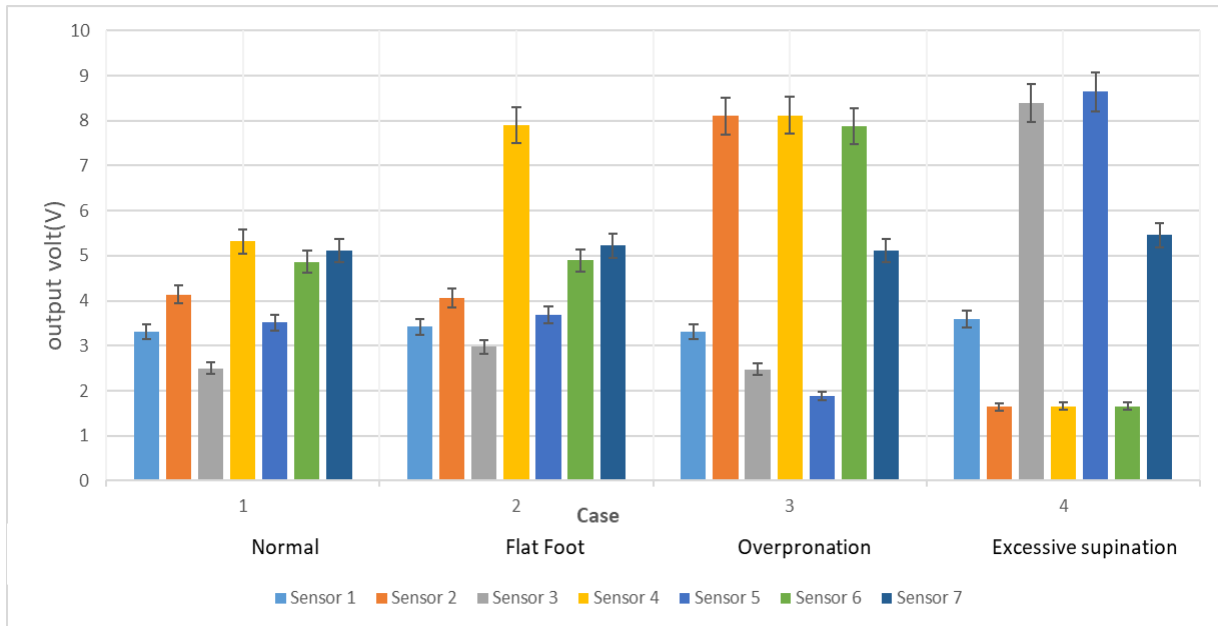


Figure 4. The numerical output of the seven sensors of all participants

Classification using FNN

The main aim of using FNN with an estimated dataset is to examine the idea of enhancing the classification using differential values of sensors and compare the performance of FNN with different ratios of testing/all data. The constructed dataset consists of 60 records, and each record contains 7 sensors value (as input for FNN) and the label of diagnosed foot cases.

During training FNN with different ratios of the dataset, the average accuracy ranges between 80% and 100% either using the raw values or differential values of sensors. The ratio of testing/all data varies between 50%, 70% and 80% which equals 30/60, 42/60 and 48/60 are samples respectively. By considering those ratios, FNN on the remaining samples was trained and then FNN was evaluated using testing samples. Training and testing of each data ratio have been done twice, the first trial has been done using raw values of sensors where the input is the raw numerical values of the seven sensors, and the second trial has been achieved using the differential values of sensors. The differential values were computed between the values of sensor #5 from the values of remained sensors which express numerically how much the values of sensors are similar or close to sensor 5 as implemented in Fig. 2. The accuracy of using FNN with testing data after finishing the training stage based on raw and differential values are illustrated in Table 4.

Table 4. The classification accuracy of the four foot cases using FNN

	Raw input		Differential input			
	50%	70%	80%	50%	70%	80%
Testin g/All data	50%	70%	80%	50%	70%	80%
Accurac y	83.33%	73.8%	62.5%	96.6%	92.8%	90%

The accuracy of testing 50% of the dataset using differential values reached 96.6% while the raw data did not exceed 83.3%. By using 70% of the dataset as testing data, an accuracy of 73.8% was obtained based on raw data and 92.8% using differential values.

On the other hand, Table 5 shows the F1-score with the same methodology of training and testing FNN. The efficient increase in the average F1-score from 64.55-85.9% using raw input to 91.40-93.30% using differential input reflects the resolution of records within the dataset for each foot case and consequently enhances the performance of FNN. Considering the four values of testing/all data ratio in Table 5, the F1-score which mostly equals 93.3% proves that differential inputs can make FNN classifies each input into the correct case.

Table 5. F1-score values of classifying the four-foot cases from samples using FNN

Raw input			
Testing/All data	50%	70%	80%
Normal	83.3%	85.71%	57.14%
Flat Foot	86.6%	88.89%	44.44%
Over-pronation	50%	83.3%	83.3%
Excessive supination	86.6%	85.71%	73.3%
Average	76.63%	85.90%	64.55%
Differential input			
Testing/All data	50%	50%	50%
Normal	93.3%	93.3%	93.3%
Flat Foot	93.3%	93.3%	93.3%
Over-pronation	93.3%	93.3%	93.3%
Excessive supination	93.3%	93.3%	93.3%
Average	93.30%	93.30%	93.30%

Compared with related work in Table 6 that use different deep learning approaches to classify the foot case using the data of plantar pressure platforms, the usual ratio of training data is at least 65% of the samples^{30, 37, 38} with classification accuracy between 99.26% and 92%. The proposed FNN with differential input reached 96.6% accuracy using 50% of samples as training data, and 90% of accuracy by using only 70% of the dataset as testing samples.

Table 6. Comparison with related work

Ref.	Foot cases	Dataset (training #, testing#)	ML model	Accuracy
30	Normal, Cavus and Planus foot	(64, 16)	1D-CNN	99.26%
37	Normal, cavus, hallux valgus	(28,13)	Multilayered backpropagation neural network	92%
38	cavus, planus	(300,200)	An adaptive neuro-fuzzy inference system	95%
Proposed work	Normal, flat, over-pronation, and excessive supination foot	(30,30)	FNN with differential input	96.6%
Proposed work	Same types	(18, 42)	FNN with differential input	90%

Discussion

In this paper, the placements of sensors (Fig. 1) showed a high variance of the numerical output from the seven sensors (Fig. 3) which makes the sensing outcomes more reliable input for a lot of machine learning tools. The placements of sensors in this study and the good resolution of voltage values corresponding to the four-foot cases and the number of participants give a new proof of the usefulness of FSR-based sensing insoles in non-invasive gait assessment. The detectable difference in average and standard deviation between flat, over-pronation, and over-pronation feet using FSR-based sensing insole is not measured previously in the related works¹⁹⁻²².

Machine learning tools come to convert non-radial types of foot diagnostics systems into self-dependent devices that can support the medical decision about the foot case or deformity²⁹⁻³². In our paper, the second main objective is to examine the idea of using differential values of sensors as input for FNN instead of using the raw data even as numerical or in “Newton” (N). The accuracy of testing all foot cases equals 83.33% using 50% of data as testing samples and this accuracy decreased to 62.5% by using only 30% of samples as training which makes the FNN unable to reach good classification performance. After using the differential input as implemented in (Fig. 2), the accuracy enhanced clearly to 96.6%

using 50% testing data, and 92.8% using 70% testing data. An 80% of the dataset was used to train 1D-CNN²⁹ with an accuracy of 99.26% to classify normal, cavus, and planus feet. In the presented work, 50% of the samples as training data was enough to get a classification accuracy of 96.6%. The comparison with related work concerning the ML approach and training/testing ratio of samples (Table 6) shows the benefit and the good impact of using the

differential values as input for neural networks and that belongs to the enhanced variance in pre-processed input compared with raw data. The idea of computing differential voltage values depends completely on determining the reference pressure point which is sensor 5 in our study. Additionally, FSR sensors can be enhanced based on micro bend multimode fiber³⁹.

Conclusion

An FSR-based sensing insole is presented to examine the normal, flat, overpronation, and excessive supination foot. The outputs of sensors show good differentiation in the values of sensors between the four-foot cases. By using differential values from sensors as input for FNN instead of using the raw data to classify the foot case, a notable increase occurred in the values of accuracy and F1-score. The efficiency of using differential input is proved by the increase in the accuracy of classification with the least amount of training data compared with testing data. The finding of this work implies the reliability of using a sensing insole in classifying the common forms of foot deformities, and the importance of considering the differential voltage between the sensing points or high-pressure points of the foot.

In future work, it is important to improve the system by increasing the number of sensors and their accuracy. In addition, conducting more experiments with different types of shoes and walking styles to evaluate the performance and robustness of the system under various conditions. Additionally, exploring other possible applications of FSR-based sensing insoles such as sports performance analysis, posture correction and fall detection. More experiments must be conducted in the near future to further validate and improve the proposed system and include individuals with a wide range of physical characteristics, foot deformities, and demographic factors to enhance the generalizability of the results.

Authors' Declaration

- Conflicts of Interest: None.
- We hereby confirm that all the Figures and Tables in the manuscript are ours. Besides, the Figures and images, which are not ours, have been given the permission for re-publication attached with the manuscript.
- Ethical Clearance: The project was approved by the local ethical committee in Al-Andalus

University and registered in the Al-Andalus University Hospital Trials Register (AUHTR0002248), and was conducted in accordance with the Declaration of Helsinki. Informed consent was obtained from all subjects involved in the study.

Authors' Contribution Statement

A.A. and H.M.N. conceptualization, methodology, data curation, software. E.I., M.A. and M.M. investigation, visualization, formal analysis,

validation, writing—original draft. A.D. supervision, project administration, resources, writing—review and editing.

Reference

1. De Groote F, Falisse A. Perspective on musculoskeletal modelling and predictive simulations of human movement to assess the neuromechanics of gait. *Proc Biol Sci.* 2021; 288(1946): 20202432. <https://doi.org/10.1098/rspb.2020.2432>
2. Sethi D, Bharti S, Prakash C. A comprehensive survey on gait analysis: History, parameters, approaches, pose estimation, and future work. *Artif Intell Med.* 2022; 129(2022): 102314. <https://doi.org/10.1016/j.artmed.2022.102314>

3. Osoba MY, Rao AK, Agrawal SK, Lalwani AK. Balance and gait in the elderly: A contemporary review. *Laryngoscope Investig Otolaryngol.* 2019; 4(1): 143-53. <https://doi.org/10.1002/liv.2.252>
4. Neves MP, da Conceição CS, Lucareli PR, da Silva Barbosa RS, Vieira JP, de Lima Brasileiro AJ, et al. Effects of Foot Orthoses on Pain and the Prevention of Lower Limb Injuries in Runners: Systematic Review and Meta-Analysis. *J Sport Rehabil.* 2022; 31(8): 1067-74. <https://doi.org/10.1123/jsr.2021-0302>
5. McClure PK, Herzenberg JE. The natural history of lower extremity malalignment. *J Pediatr Orthop.* 2019 J; 39(6): S14-9. <https://doi.org/10.1097/BPO.0000000000001361>
6. Douglas C, Wright J, Jacobs B. Variations in gait development: what is normal and when should I be concerned?. *Paediatr Child Health.* 2022; 32(2): 71-6. <https://doi.org/10.1016/j.paed.2021.11.005>
7. Collins C. Getting Ready for Foot Care Certification: Foot Care Basics: Foot Care Basics. *J Wound Ostomy Continence Nurs.* 2019; 46(3): 248-50. <https://doi.org/10.1097/WON.0000000000000531>
8. Jiang H, Mei Q, Wang Y, He J, Shao E, Fernandez J, Gu Y. Understanding foot conditions, morphologies and functions in children: a current review. *Front Bioeng Biotechnol.* 2023; 11(2023): 1192524. <https://doi.org/10.3389/fbioe.2023.1192524>
9. Arachchige SN, Chander H, Knight A. Flatfeet: Biomechanical implications, assessment and management. *Foot.* 2019; 38(2019): 81-5. <https://doi.org/10.1016/j.foot.2019.02.004>
10. Hadj-Moussa F, Ngan CC, Andrysek J. Biomechanical factors affecting individuals with lower limb amputations running using running-specific prostheses: A systematic review. *Gait Posture.* 2022; 92: 83-95. <https://doi.org/10.1016/j.gaitpost.2021.10.044>
11. Zhang B, Lu Q. A current review of foot disorder and plantar pressure alternation in the elderly. *Phys Act Health.* 2020; 4(1): 95. <https://doi.org/10.5334/paah.57>
12. Osher L, Shook JE. Imaging of the Pes cavus deformity. *Clin Podiatr Med Surg.* 2021; 38: 303-21. <https://doi.org/10.1016/j.cpm.2021.03.004>
13. Ortolani M, Leardini A, Pavani C, Scicolone S, Girolami M, Bevoni R, et al. Angular and linear measurements of adult flexible flatfoot via weight-bearing CT scans and 3D bone reconstruction tools. *Sci Rep.* 2021; 11(1): 16139. <https://doi.org/10.1038/s41598-021-95708-x>
14. Ahmad AA, Ghanem AF, Hamaida JM, Maree MS, Aker LJ, Kamesh MI, et al. Magnetic resonance imaging of severe idiopathic club foot treated with one-week accelerated Ponseti (OWAP) technique. *Foot Ankle Surg.* 2022; 28(3): 338-46. <https://doi.org/10.1016/j.fas.2021.04.012>
15. Alsabek MB, Abdul Aziz AR. Diabetic foot ulcer, the effect of resource-poor environments on healing time and direct cost: A cohort study during Syrian crisis. *Int Wound J.* 2022; 19(3): 531-7. <https://doi.org/10.1111/iwj.13651>
16. Tan AM, Fuss FK, Weizman Y, Woudstra Y, Troynikov O. Design of low cost smart insole for real time measurement of plantar pressure. *Procedia Technol.* 2015; 20(2015): 117-22. <https://doi.org/10.1016/j.protcy.2015.07.020>
17. Ren B, Liu J. Design of a Plantar Pressure Insole Measuring System Based on Modular Photoelectric Pressure Sensor Unit. *Sensors.* 2021;21(11):3780. <https://doi.org/10.3390/s21113780>
18. Zhang Q, Wang YL, Xia Y, Wu X, Kirk TV, et al. A low-cost and highly integrated sensing insole for plantar pressure measurement. *Sens BioSensing Res.* 2019; 26(2019): 100298. <https://doi.org/10.1016/j.sbsr.2019.100298>
19. Fazio R, Perrone E, Velázquez R, De Vittorio M, Visconti P. Development of a self-powered piezo-resistive smart insole equipped with low-power BLE connectivity for remote gait monitoring. *Sensors.* 2021; 21(13): 4539. <https://doi.org/10.3390/s21134539>
20. Wang W, Cao J, Yu J, Liu R, Bowen CR, et al. Self-powered smart insole for monitoring human gait signals. *Sensors.* 2019 ;19(24): 5336. <https://doi.org/10.3390/s19245336>
21. Park J, Kim M, Hong I, Kim T, Lee E, Kim E-A, et al. Foot plantar pressure measurement system using highly sensitive crack-based sensor. *Sensors.* 2019; 19(24). <https://doi.org/10.3390/s19245504>
22. Suprpto SS, Setiawan AW, Zakaria H, Adiprawita W, Supartono B. Low-cost pressure sensor matrix using velostat. 2017 5th International Conference on Instrumentation, Communications, Information Technology, and Biomedical Engineering (ICICI-BME), IEEE; 2017. <https://doi.org/10.1109/ICICI-BME.2017.8537720>
23. López DL, González LC, Iglesias ME, Canosa JL, Sanz DR, Lobo CC, et al. Quality of Life Impact Related to Foot Health in a Sample of Older People with Hallux Valgus. *Aging Dis.* 2016;7 (1):45-52. <https://doi.org/10.14336/AD.2015.0914>
24. Subramaniam S, Majumder S, Faisal AI, Deen MJ. Insole-based systems for health monitoring: Current solutions and research challenges. *Sensors.* 2022; 22(1): 438. <https://doi.org/10.3390/s22020438>
25. Wang M, Wang X, Fan Z, Chen F, Zhang S, Peng C. Research on feature extraction algorithm for plantar pressure image and gait analysis in stroke patients. *J Vis Commun Image Represent.* 2019; 58(2019): 525-31. <https://doi.org/10.1016/j.jvcir.2018.12.017>
26. Chae J, Kang Y-J, Noh Y. A Deep-Learning Approach for Foot-Type Classification Using Heterogeneous Pressure Data. *Sensors.* 2020; 20(16):4481. <https://doi.org/10.3390/s20164481>

27. Rosero-Montalvo PD, Fuentes-Hernández EA, Morocho-Cayamcela ME, Sierra-Martínez LM, Peluffo-Ordóñez DH. Addressing the data acquisition paradigm in the early detection of pediatric foot deformities. *Sensors*. 2021; 21(13):4422. <https://doi.org/10.3390/s21134422>
28. Mun F, Choi A. Deep learning approach to estimate foot pressure distribution in walking with application for a cost-effective insole system. *J Neuroeng Rehabil*. 2022; 19(1): 4. <https://doi.org/10.1186/s12984-022-00987-8>
29. Mei Z, Ivanov K, Zhao G, Wu Y, Liu M, Wang L. Foot type classification using sensor-enabled footwear and 1D-CNN. *Measurement*. 2020; 165(2020): 108184. <https://doi.org/10.1016/j.measurement.2020.108184>
30. Balbin JR, De Guzman JPB, Trinidad JGN, Yaya FDS. Foot deformity determination and health risk prediction through foot plantar analysis using pressure sensor matrix. 2021 IEEE International Conference on Automatic Control & Intelligent Systems (I2CACIS), IEEE; 2021. <https://doi.org/10.1109/I2CACIS52118.2021.9495907>
31. D'Angelantonio E, Lucangeli L, Camomilla V, Mari F, Mascia G, Pallotti A. Classification-Based Screening of Phlebopathic Patients Using Smart Socks. Proceedings of the 2021 IEEE International Symposium on Medical Measurements and Applications (MeMeA), IEEE; n.d. <https://doi.org/10.1109/MetroInd4.0IoT54413.2022.9831481>
32. Chen M, Huang B, Xu Y. Postural kyphosis detection using intelligent shoes. 2008 IEEE International Conference on Robotics and Automation, IEEE; 2008. <https://doi.org/10.1109/ROBOT.2008.4543658>
33. Ghani APDRF, Hassan HS. Human Computer Interface for Wheelchair Movement. *Baghdad Sci J*. 2017; 14(2): 0437. <https://doi.org/10.21123/bsj.2017.14.2.0437>
34. Florez JA, Velasquez A. Calibration of force sensing resistors (fsr) for static and dynamic applications. 2010 IEEE ANDESCON, IEEE; 2010. <https://doi.org/10.1109/ANDESCON.2010.5633120>
35. Queen RM, Mall NA, Hardaker WM, Nunley JA. Describing the medial longitudinal arch using footprint indices and a clinical grading system. *Foot Ankle Int*. 2007; 28(4): 456–62. <https://doi.org/10.3113/fai.2007.0456>
36. Domínguez-Morales MJ, Luna-Perejón F, Miró-Amarante L, Hernández-Velázquez M, Sevillano-Ramos JL. Smart footwear insole for recognition of foot pronation and supination using neural networks. *Appl Sci*. 2019; 9(19): 3970. <https://doi.org/10.3390/app9193970>
37. Barton JG, Lees A. Development of a connectionist expert system to identify foot problems based on under-foot pressure patterns. *Clin Biomech*. 1995; 10(7): 385–91. [https://doi.org/10.1016/0268-0033\(95\)00015-d](https://doi.org/10.1016/0268-0033(95)00015-d)
38. Xu S, Zhou X, Sun Y-N. A novel gait analysis system based on adaptive neuro-fuzzy inference system. *Expert Syst Appl*. 2010; 37(2): 1265–9. <https://doi.org/10.1016/j.eswa.2009.06.026>
39. AL-Dabagh samar Y, ALjaber NA, AL-Hassnawy GO. Designing and Constructing the Strain Sensor Using Microbend Multimode Fiber . *Baghdad Sci J*. 2018; 15(2): 0217. <https://doi.org/10.21123/bsj.2018.15.2.0217>

كشف تشوهات القدم المختلفة باستخدام حساسات الضغط الأومية وتصنيفها سكونيا من خلال الشبكات العصبونية

أيهم درويش^{1,2}، ابراهيم اسماعيل¹، أيمن الكيال¹، مجتبي علي¹، محمد مصري¹، حسن محمد نزهة³

¹كلية الهندسة الطبية، جامعة الأندلس للعلوم الطبية، طرطوس، سورية.

²قسم الأتمتة الصناعية، كلية الهندسة التقنية، جامعة طرطوس، طرطوس، سورية.

³قسم الميكانيكا، كلية الهندسة الميكانيكية، جامعة أوتو فون جويريك، ماغديبورغ، ألمانيا.

الخلاصة

تُعد أنظمة النعال الحساسة للحركة تقنية واعدة للعديد من التطبيقات في الرعاية الصحية والرياضة. حيث يمكن أن توفر هذه الأنظمة معلومات قيمة حول توزيع الضغط على القدم وأنماط المشي لأفراد مختلفين. ومع ذلك، فإن تصميم وتنفيذ مثل هذه الأنظمة يواجه العديد من التحديات، مثل اختيار الحساسات والمعايرة ومعالجة البيانات والتفسير. في هذه الدراسة، نقتراح نظام نعل حساس باستخدام مقاومات استشعار القوى لقياس الضغط المطبق من القدم على مناطق مختلفة من النعل. يقوم هذا النظام بتصنيف أربعة أنواع من تشوهات القدم: طبيعي، مسطح، انحراف القدم إلى الداخل، وزيادة انحراف القدم إلى الخارج. تستخدم مرحلة التصنيف قيم الضغط الفرقية على نقاط الضغط كمدخلات لنموذج التغذية الأمامية للشبكات العصبونية. تم جمع البيانات من 60 فرداً تم تشخيصهم بالحالات المدروسة. حقق تنفيذ التغذية الأمامية للشبكات العصبونية دقة بنسبة 96.6% باستخدام 50% من المجموعة البيانية كبيانات تدريبية و 92.8% باستخدام 30% من البيانات التدريبية فقط. ويوضح المقارنة مع الأعمال ذات الصلة الأثر الإيجابي لاستخدام القيم الفرق لنقاط الضغط كمدخلات للشبكات العصبونية مقارنة بالبيانات الأولية.

الكلمات المفتاحية: تشوهات القدم، التغذية الأمامية للشبكات العصبونية، مشية الإنسان، مقاوم استشعار القوة، النعال الحساسة.